

Raman spectra of carbon nanotubes and nanofibers prepared by ethanol flames*

YUELI LIU, CHUNXU PAN[‡], JIANBO WANG

Department of Physics, Wuhan University, Wuhan 430072, People's Republic of China; Center for Electron Microscopy, Wuhan University, Wuhan 430072, People's Republic of China
E-mail: cxpan@whu.edu.cn

Laser Raman analysis is an important method for studying carbon nanotubes (CNTs) and carbon nanofibers (CNFs), which provides information of CNTs and CNFs such as vibration of crystal lattice, electron structure and integrity of crystal structure, etc. [3–5]. Regularly, three methods are commonly used to synthesize CNTs, i.e., electric arc-discharge [6], laser ablation [7], chemical vapor deposition (CVD) [8] (or called catalytic pyrolysis [9]), etc., and one method to prepare the so-called vapor-grown CNFs [10, 11]. In our previous work [1, 2], a novel method by using liquid ethanol flames was successfully used to synthesize CNTs. Comparing with other methods, the present process used flame to synthesize the CNTs or CNFs in the atmosphere and it might adopt different catalysis-growth mechanisms. Therefore, it is necessary to investigate the characteristics of the Raman spectra of the synthesized materials.

The experiment utilized the common combustion apparatus for ethanol flames. The substrate materials are Type 304 austenitic stainless steel (18.5 wt% Cr, 9.0 wt% Ni and Bal. Fe) and low carbon mild steel (0.12 wt% C, 0.45 wt% Mn, 0.30 wt% Si, 0.045 wt% P, 0.030 wt% S and Bal. Fe). The sampling surfaces of the substrates need to be pre-treated by mechanical polishing and then dipped in pure nitric acid (HNO₃) solution for 0.5 to 2 min, which was supposed to generate small particles on the surfaces for catalyzing growth of CNTs or CNFs. The detailed synthesis process has been described in our previous work [1, 2]. The combustion products on the substrates were then used for laser Raman spectrum and electron microscopic examinations.

Microstructures and morphologies of CNTs and CNFs are observed by using Japan Hitachi S-570 scanning electron microscope (SEM), Japan Jeol JEM 2010 conventional transmission electron microscope (TEM) and Jeol JEM 2010FEF high-resolution transmission electron microscope (HRTEM), respectively. The laser Raman spectra were performed in an England Renishaw-1000 laser Raman spectroscopy instrument in the back-scattering configuration at room temperature. The excitation source is 514.5 nm Ar-ion laser line. The laser line is in the range of 80–4500 cm⁻¹. The laser beam uses a microscope objective of ×50.

The spectral resolution is 3 cm⁻¹. And the optical power at the sample is maintained at 5 mW.

Generally, the SEM morphologies of the combustion products were fibrillous structures, which grew erectly or disorderly and randomly [1, 2]. Further TEM and HRTEM observations indicated that these fibers showed quite different inner structures when grown on the different substrates, i.e., the combustion materials from the sampling surface of modified Ni-contained austenitic stainless steel substrate mostly have hollow-centered structures with well ordered graphitic layers, as shown in Fig. 1, which correspond to the CNTs. However, the products from low carbon mild steel substrates showed a kind of solid-cored structure, and some have spiral structures, which are named as CNFs. These CNFs are completely different from the so-called vapor-grown carbon nanofibers (VGCNFs) [10, 11]. HRTEM observation illustrated that the CNFs have disordered graphitic layers, as shown in Fig. 2.

Fig. 3 illustrates the Raman spectra of the combustion products from different substrates and Table I lists the differences in parameters. Obviously, the major differences lie in the intensity of the peaks located at 2695 cm⁻¹ and the values of ratio I_D/I_G , which are related to the graphitic structures of the combustion materials.

It is well known that the sp^2 carbon atoms form three covalent bonds and make the carbon atoms combine into a plane of hexangular reticulation structure. Theoretically, CNTs are considered to be rolled from two-dimensional graphite sheets, that is, a single-walled carbon nanotube (SWCNT) is formed from only one graphite sheet, and a multi-walled carbon nanotube (MWCNT) is from several graphite sheets. The analysis of Raman spectra of CNTs is based on phonon dispersion relationship of two-dimensional graphite, and the method of folding of the Brillouin zone. Generally, the first-order Raman spectrum is determined by the vibration modes near the center of Brillouin zone. The main peaks corresponding to the carbon materials are listed below:

(1) 1550–1600 cm⁻¹ is the graphite band (*G*-band) which is produced from the high degree of symmetry

*The present work is a continuation on the synthesis of carbon nanotubes (CNTs) by using ethanol flame [1, 2].

[‡]Author to whom all correspondence should be addressed.

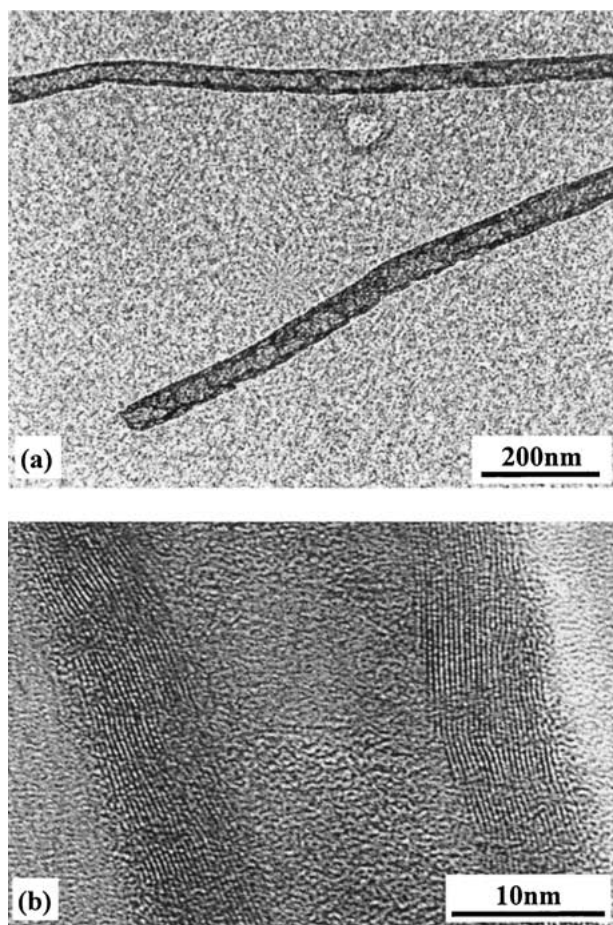


Figure 1 Micrographs of CNTs grown on austenitic stainless steel substrate: (a) TEM image and (b) HRTEM image.

and order of carbon materials, and generally used to identify well-ordered CNTs [3–5];

(2) $1250\text{--}1450\text{ cm}^{-1}$ is the disorder-induced phonon mode (D -band), which is related to the mode of boundaries in Brillouin zone. It is caused from the disordered components, and mainly originated from phonon mode of M -point and K -point of the hexagonal Brillouin zone. It has a high sensitivity to the disordered structures in carbon materials [3–5];

(3) $2500\text{--}2900\text{ cm}^{-1}$ is the second order D -band (or called D^* -band), which is related to the boundary point K in Brillouin zone of graphite and depended upon the packing in three-dimensional space [12]. Therefore, the relative intensity value I_D/I_G (or I_{D^*}/I_G) can also be used to characterize the degree of order of carbon materials, i.e., Smaller ratio of I_D/I_G or larger ratio of I_{D^*}/I_G corresponding to the higher order degree of substances, such as CNTs;

(4) The peaks at 2875 cm^{-1} , 2987 cm^{-1} and 3146 cm^{-1} are due to symmetric and asymmetrical

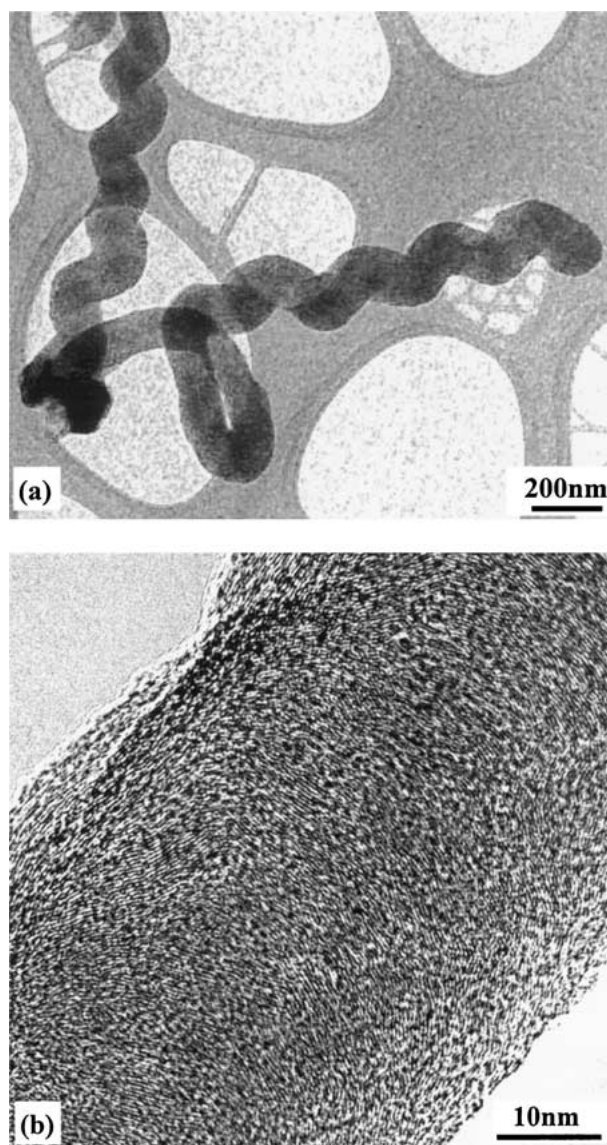


Figure 2 Micrographs of CNFs grown on low carbon mild steel substrates: (a) TEM image and (b) HRTEM image.

$C\text{--}H$ stretch vibrations of the CH_3 group and asymmetrical $C\text{--}H$ stretch vibrations of the CH_2 group, respectively [13].

According to the above discussions, the larger D^* peak and smaller I_D/I_G ratio or larger I_{D^*}/I_G ratio in Fig. 3a indicate that the combustion products on the Ni-contained austenitic stainless steel substrate have higher degrees of order and graphitization than those on the low carbon mild steel substrate. These results just coincide with the observations from TEM and HRTEM, as shown in Figs 1 and 2. This means that austenitic stainless steel tends to be a substrate to synthesize CNTs, while the low carbon mild steel yields

TABLE I Laser Raman spectra parameters of CNTs and CNFs

	D -band (cm^{-1})	G -band (cm^{-1})	D^* -band (cm^{-1})	I_D/I_G
CNTs	1355	1582	2694	0.90
CNFs	1350	1592	2699	1.24
Comparisons of frequency shift between the CNTs and CNFs	Blue shift 5 cm^{-1}	Red shift 10 cm^{-1}	Red shift 5 cm^{-1}	

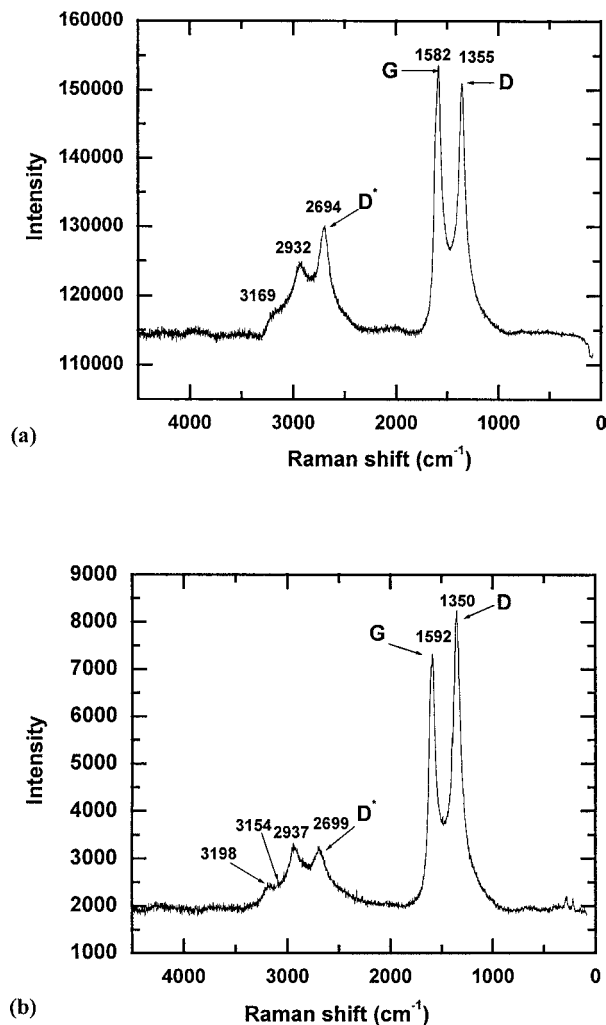


Figure 3 Typical laser Raman spectra: (a) CNTs on stainless steel substrate and (b) CNFs on low carbon mild steel substrate.

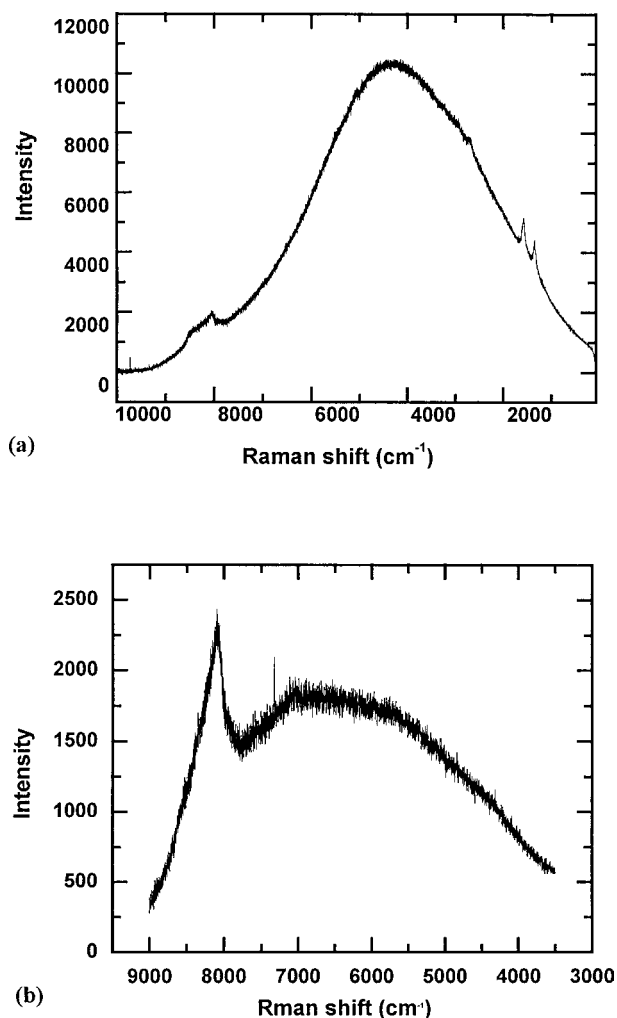


Figure 4 Laser Raman fluorescence spectra: (a) CNTs on stainless steel substrate and (b) CNFs on low carbon mild steel.

only CNFs, which also implied that the formation of solid-cored CNFs was related to the element Fe or its compounds, and CNTs related to Ni or its compounds. The detailed mechanisms need to be discussed further.

In addition, the Raman “red shift” in *G* and *D** bands and “blue shift” in *D* band in Table I are caused due to the differences between CNTs and CNFs microstructures, such as the quantum-size effect of CNTs with “hollow-centered” and the diameter differences.

When compared with the Raman spectra of CNTs synthesized from other methods, such as electric arc-discharge [4] and CVD [6], the present Raman spectra obviously give the larger intensity of *D* band. This shows that the CNTs from the flame have large numbers of disorder structures or defects [14, 15], which perhaps is related to its unique synthesis conditions in the atmosphere and carbon source.

Experiments also found that either CNTs or CNFs have a parabolic curve in the side of high Raman shift range 3500 to 10000 cm^{-1} , as shown in Fig. 4, which belong to the laser-induced fluorescence spectra. Generally, the fluorescence phenomenon is caused by the transition between electron energy bands, which can be simply described as a laser-absorbed radiation of an atom or molecule system. Further research on the phenomenon is being undertaken.

It is concluded that the CNTs grown on stainless steel substrates possess higher graphitic degree of order than the CNFs on mild steel substrates during ethanol flaming synthesis, according to both HRTEM microstructural observations and Raman scattering analysis. However, the fluorescence phenomenon found in the Raman spectra may indicate that the present method induces more defects or impurities in the CNTs and CNFs, due to the synthesis process in atmosphere, when compared with the other methods. The present work may hint that the flame synthesized CNTs and CNFs can be used as novel photoluminescence materials in future applications.

Acknowledgments

This work was supported by the Mr. Shao Yi Zhou Research Foundation of Wuhan University, and the Scientific Research Foundation for the Returned Overseas Chinese Scholars, State Education Ministry.

References

1. C. PAN and X. XU, *J Mater. Sci. Lett.* **21** (2002) 1027.
2. C. PAN and Q. BAO, *ibid.* **21** (2002) 1927.
3. W. Z. LI, H. ZHANG, C. Y. WANG, Y. ZHANG, L. W. XU, K. ZHU and S. S. XIE, *Appl. Phys. Lett.* **70** (1997) 2684.

4. P. C. EKLUND, J. M. HOLDEN and R. A. JISHI, *Carbon* **33** (1995) 959.
5. M. S. DRESSELHAUS, G. DRESSELHAUS, A. JORIO, A. G. SOUZA FILHO and R. SAITO, *ibid.* **40** (2002) 2043.
6. Y. ANDO, X. ZHAO, S. INOUE and S. IJIMA, *J. Cryst. Growth* **237–239** (2002) 1926.
7. A. THESS, R. LEE, P. NIKOLAEV, H. J. DAI, P. PETIT, J. ROBERT, C. H. XU, Y. H. LEE, S. G. KIM, A. G. R. INZLER, D. T. COLBERT, G. E. SCUSERIA, D. TOMANEK, J. E. FISCHER and R. E. SMALLEY, *Science* **273** (1996) 483.
8. C. SINGH, M. S. P. SHAFFER and A. H. WINDLE, *Carbon* **41** (2003) 359.
9. A. M. BENITO, Y. MANIETTE, E. MUNOZ and M. T. MARTINEZ, *ibid.* **36** (1998) 681.
10. Y. Y. FAN, H. M. CHENG, Y. L. WEI, G. SU and Z. H. SHEN, *ibid.* **38** (2000) 789.
11. *Idem.*, *ibid.* **38** (2000) 921.
12. C. PAN and Q. BAO, *J. Mater. Sci. Lett.* **21** (2002) 1927.
13. T. C. CHIEU, M. S. DRESSELHAUS and M. ENDO, *Phys. Rev. B* **26** (1982) 5867.
14. H. B. ZHANG, G. D. LIN, Z. H. ZHOU, X. DONG and T. CHEN, *Carbon* **40** (2002) 2429.
15. W. S. BACSA, D. UGARATE, A. CHATELAIN and W. A. DE HEER, *Phys. Rev. B* **50** (1994) 15473.
16. P. TAN, G. YU, F. HUANG, S. ZHANG, Z. SHI, X. ZHOU and Z. GU, *Chin. J. Light Scatter.* **8**(3) (1996) 125 (in Chinese).

*Received 8 May
and accepted 14 August 2003*